J. Phys. Chem. **1986**, *90*, 375-383

Laser Stimulation and Observation of Bimolecular Reactions

J. Wolfrum

Physikalisch-Chemisches Institut der Ruprecht-Karls-Universität, D-6900 Heidelberg, F.R.G.
(Received: July 22, 1985)

The paper describes the results of experiments on the effect of selective translational, rotational, vibrational, and electronic excitation of reactants in bimolecular reactions using flow systems, crossed molecular beams, UV- and IR-laser excitation, and reactant and product detection by time-resolved atomic line resonance absorption, mass spectrometry, LIF, and CARS. The experimental results are compared with the results of quantum and quasiclassical trajectory studies on ab initio potential surfaces and with thermal rate parameters.

Introduction

Conventionally, the energy dependence of a chemical reaction rate is studied under conditions in which the rate of reaction is slow compared to that of collisional energy transfer. Under these conditions, the energy of the reactants is characterized by a temperature. The Arrhenius parameters obtained in this way, however, contain no direct information on how the various degrees of freedom of the reacting molecules and of the "activated complex" contribute to overcoming the potential barriers of product formation in the chemical reaction. Investigations on the chemical reactivity under a wide range of conditions such as specific excitation of the reactants therefore give an important insight into the microscopic dynamics of the chemical reaction. This information can be compared with the results of theoretical predictions using potential energy hypersurfaces for chemical reactions obtained by "ab initio" methods and is also of fundamental interest in improving kinetic data for practical applications such as detailed chemical kinetic modeling studies.

The experimental possibilities for studying elementary chemical reactions in detail have expanded quite dramatically in recent years as a result of the development of various laser sources. The coherence, collimation, monochromaticity, polarization, tunability, and short pulse duration of laser light now available in the infrared, visible, and ultraviolet regions allow the preparation and detection of chemically reacting molecules with an unprecedented degree of selectivity. The present paper discusses experimental and theoretical investigations on the effect of selective translational, rotational, vibrational, and electronic excitation of the reactants.

Translational Excitation

The technique of flash or atomic resonance line photolysis for the production of hot atoms in conjunction with time-integrated product detection methods has long been used to obtain information about relative reaction cross sections and excitation functions as a function of the translational energy of the reactants. In these experiments, the measured reaction yields could only be used to calculate reaction probabilities or cross sections, with estimations of the collisional cooling process of the hot particles. The use of pulsed lasers to produce translationally hot atoms or radicals by photofragmentation of small molecules in combination with fast time-resolved product detection techniques such as laser-induced fluorescence (LIF), multiphoton ionization (MPI), or coherent anti-Stokes Raman spectroscopy (CARS) allows product detection under approximately single-collision conditions. Detailed product-state distributions and absolute total reaction cross sections can be obtained in this way.[1] These microscopic data can be compared with dynamic calculations using ab initio potential energy surfaces.

TABLE I

	$H + H_2O$	$H + CO_2$	$H + O_2$
$E_{\mathrm{coll}}^{\mathrm{c.m.}}$, kcal/mol	58.2	60.1	60.7
σ, Å^2	0.24 ± 0.1	0.37 ± 0.1	0.42 ± 0.2
$\sigma(\nu{=}1)/\sigma(\nu{=}0)$	≤0.1	≤0.1	0.47 ± 0.15
$[\sigma(^2\Pi_{3/2})/\sigma(^2\Pi_{1/2})]\cdot[N/(N+1)]$	1.1 ± 0.2	1.2 ± 0.2	1.2 ± 0.2
$\sigma(\Pi^+)/\sigma(\Pi^-)$	3.2 ± 1.0	3.0 ± 1.0	5.9 ± 1.0

The experimental apparatus used has been described in detail elsewhere.[1,2] Two antiparallel laser beams are directed coaxially through a flow reactor equipped with a baffle system to reduce the scattered light from the excimer laser photolysis pulse and from the excimer laser pumped dye laser analysis pulse. The dye laser operates with rodamine 640 and a frequency doubling KDP crystal to generate a pulse in the 306–311-nm region to probe $OH(^2\Pi)$ radicals by laser-induced fluorescence. Fluorescence light is then detected as a function of the dye laser wavelength, after passing through emission optics and a filter transmitting between 240 and 390 nm, by a photomultiplier. The photomultiplier current is measured by a boxcar integration system. The timing sequence of the laser pulses was governed by a central clock, which starts both excimer laser discharges with a continuously adjustable time delay. As examples, experimental and theoretical results for the elementary reaction system

$$H + O_2 \rightleftarrows OH + O \quad (1)$$

$$H + CO_2 \rightleftarrows CO + OH \quad (2)$$

$$H + H_2O \rightleftarrows H_2 + OH \quad (3)$$

are discussed here.

Figure 1 gives nascent rotational state distributions for the reactions at relative collision energies of 250 kJ/mol. Despite the comparable total reaction energies, the nascent $OH(v{=}0)$ rotational distributions are quite different. The distribution from the $H + O_2$ reaction is extremely hot, broadly peaked at rotational quantum numbers around $N = 11$ in the $H + CO_2$ case, and restricted to low values with only 3% of the total available energy partitioned into rotation for the $H + H_2O$ system. The observed rotational energy distributions give interesting microscopic details on the molecular dynamics of these elementary steps. Spin–orbit and orbital–rotation interactions in the OH radical cause fine-structure splittings for each rotational level. Each of these fine structure levels can be probed by different rotational subbands. As shown in Table I, the two OH spin states $^2\Pi_{1/2}$ and $^2\Pi_{3/2}$ are, within experimental error, equally populated. However, the Λ-doublet fine structure states show a clear preference for the lower-energy Π^+ component. The experimental results show that breakup of the reaction complex generates forces in a plane containing the bond to be broken. The OH radical rotates in that plane and J_{OH} is perpendicular to it and to the broken bond. This picture is consistent only with a preferential planar exit channel in these reactions. This could also be directly demonstrated by using polarized photolysis and analysis laser beams.

The experimental apparatus is shown in Figure 2. Here, both lasers were linearly polarized (around 95% polarization) by using 10 Brewster quartz plates respectively (rack polarizer). Both light

---

(1) K. Kleinermanns and J. Wolfrum, *J. Chem. Phys.*, **80**, 1446 (1984).
(2) K. Kleinermanns and J. Wolfrum, *Appl. Phys. B*, **34**, 5 (1984).

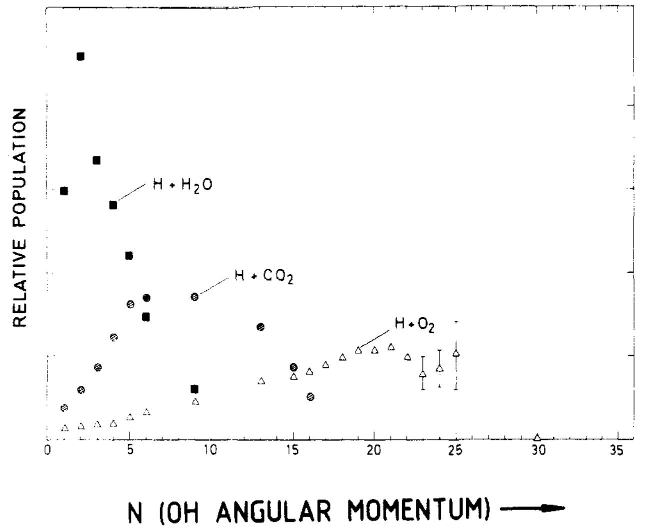

Figure 1. Nascent rotational state distributions in OH(v=0) formed in the reactions 1–3 at 250 kJ/mol relative collision energy.

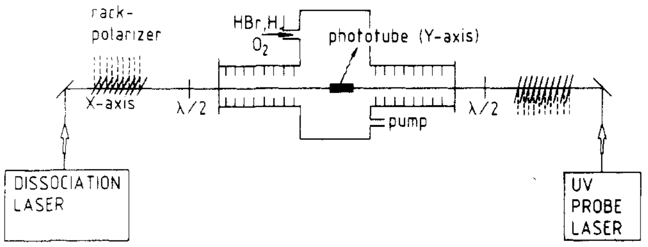

Figure 2. Experimental arrangement for the observation of reaction product spatial rotational alignment as a function of the atom flight direction.

beams are then directed through $\lambda/2$ plates so that the electric vectors of both lasers can be adjusted to any desired angle independently.

The polarization experiments are based on measuring the distribution of orientations of the OH angular momentum vector **J** by using polarized dissociation and analysis lasers. The OH-radical fluorescence intensity is observed with the electric vectors of both lasers E_D and E_E parallel and perpendicular to each other. The cases (a) $E_E \| E_D \| Z$ and (b) $E_E \perp E_D \| Z$, with the lasers propagating along X and the phototube along Y, are used. The polarization ratio R is defined as the ratio of the fluorescence intensity in case a to that in case b. R is measured as function of J for Q branch transitions, because here μ_{OH} lies along J_{OH} and larger polarization effects are expected. For P or R transitions, μ_{OH} is perpendicular to J_{OH} and rotates in the OH plane[4] of rotation.

Dissociation of HBr at 193 nm to H + Br($^2P_{3/2}$) is induced by a perpendicular transition, so that the H atom flight direction is aligned with a $\sin^2 \theta$ distribution along E_D, i.e. preferentially $v_H \perp E_D$. Interesting information on H–O_2 reaction dynamics can be obtained by investigating possible memory effects of OH product alignment on reactant alignment. Figure 3 shows the variation of the OH-$Q_1$16 (v'' = 0) fluorescence intensity with polarization of the dissociation laser E_D relative to analysis laser E_E. We assume the observed preference $J_{OH} \| E_D \perp v_H$ to be due to restrictions in the possible reaction geometries at high collision energies. Λ-doublet measurements and trajectory calculations suggest that the H + O_2 reaction occurs essentially in a plane at high collision energies. From that we expect $J_{OH} \perp v_H$ for randomly oriented O_2 molecules.[5] The transition moment μ_E of Q lines is perpendicular to the OH rotation plane ($\| J_{OH}$) for high OH rotational states. Thus we obtain the maximum OH excitation probability $|E_E \mu_E|^2$ for $\mu_Q \| E_E \| J_{OH} \perp v_H$ resulting in higher fluorescence intensity for $E_E \| E_D$ than for $E_E \perp E_D$. The model is quantitatively described elsewhere.[3] The surprisal analysis of the rotational distributions in OH(v''=0) with H atoms from HBr (2.6 eV) and HI photolysis (E = 1.9 and 1.0 eV) gives straight lines with θ_R = +1.2, −0.7, and −1.2 at E = 1.0, 1.9, and 2.6 eV, respectively. All three slopes are quite small compared to those of other "nonstatistical" reactions.[6]

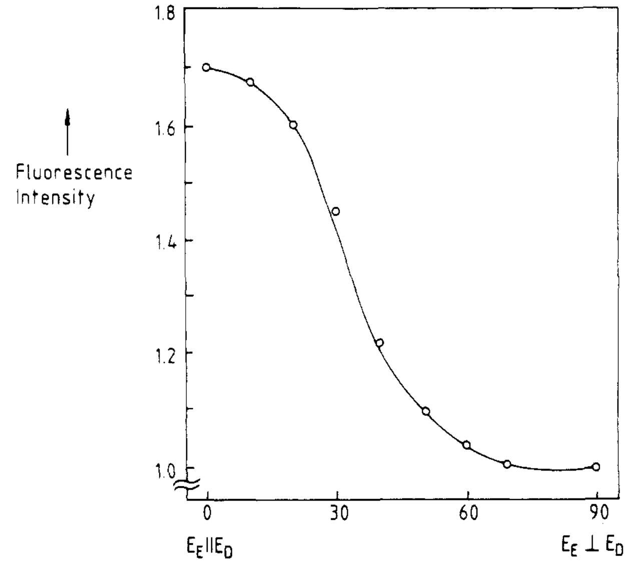

Figure 3. Variation of the OH-$Q_1$16 (v'' = 0) fluorescence intensity from reaction 1 with polarization of the dissociation laser E_D relative to the analysis laser E_E.

Reaction 1 is known to take place adiabatically on the ground-state potential surface of the HO_2($^2A''$) radical. Trajectory calculations[5] on an ab initio surface (Melius–Blint[7]) are in agreement with calculated OH rotational distributions from the phase space theory[8] for low relative translational energy. With increasing relative translational energy the OH rotational distribution becomes considerably hotter than the statistical one, and no long living HO_2 complex exists during the reaction. An total reaction cross section of 0.42 ± 0.2 Å^2 at E = 2.6 eV is obtained for reaction 1 in the experiments described here. The theoretical cross section obtained under this condition by quasiclassical trajectory calculations[5,9] on the Melius–Blint surface is 0.38 Å^2. These numbers cannot be compared directly, because the multiplicity of the $^2A''$ surface at infinite H–O_2 separation is not taken into account. Miller[9] uses a multiplicity factor of $^1/_3$. This would yield a theoretical cross section of 0.13 Å^2 which is significantly outside the experimental range (see Figure 4a). Calculated rate coefficients obtained by using this theoretical cross section[9] are in agreement with shock tube measurements of the rate of reaction 1 by Schott[10] and Chiang and Skinner.[10] However, as shown in Figure 4b, recent shock tube experiments by Just and Frank[11] using time-resolved atomic resonance line absorption coincide with the extrapolated values recommended by Baulch et al.[12] Even higher rate data for k_1 are reported by Bowman.[13] In the recombination pathway

$$H + O_2 \rightarrow HO_2{}^* \xrightarrow{+M} HO_2 \qquad (1a)$$

---

(3) K. Kleinermanns and E. Linnebach, *Appl. Phys. B*, **36**, 203 (1985).

(4) M. P. Sinka, C. D. Caldwell, and R. N. Zare, *J. Chem. Phys.*, **61**, 491 (1974). D. A. Case, G. M. McClelland, and D. R. Herschbach, *Mol. Phys.*, **35**, 541 (1978).

(5) K. Kleinermanns and R. Schinke, *J. Chem. Phys.*, **80**, 1440 (1984).

(6) A. C. Luntz, *J. Chem. Phys.*, **73**, 5394 (1980). J. Silver, W. Dipfl, J. Brophy, and J. Kinsey, *J. Chem. Phys.*, **65**, 1811 (1976).

(7) C. F. Melius and R. J. Blint, *Chem. Phys. Lett.*, **64**, 183 (1979).

(8) P. Pechukas, J. C. Light, and C. Rankin, *J. Chem. Phys.*, **44**, 794 (1966).

(9) J. A. Miller, *J. Chem. Phys.*, **74**, 5120 (1981).

(10) G. L. Schott, *Combust. Flame*, **21**, 357 (1973).

(11) Th. Just and P. Frank, *Ber. Bunsenges. Phys. Chem.*, **89**, 181 (1985).

(12) D. L. Baulch, D. D. Drysdale, and D. G. Horne, *Symp. (Int.) Combust.*, [*Proc.*], *14th*, *1972*, 107 (1973).

(13) C. T. Bowman, *Symp. (Int.) Combust.*, [*Proc.*], *15th*, *1974*, 869 (1975).

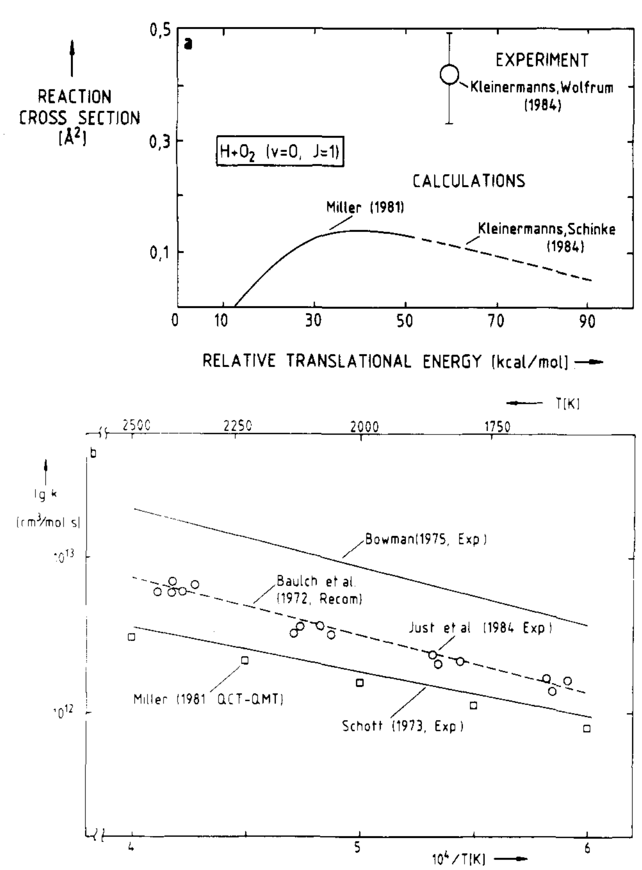

Figure 4. (a) Calculated and measured reactive cross sections for reaction 1. (b) Measured (○) and calculated (□) thermal rates for the reaction 1 (see text).

new measurements of the high-pressure-limit recombination rate coefficient[14] also are higher than calculated values.[15] The observed discrepancies could be attributed to a reduction of calculated reaction cross sections due to a "rigid" character and a barrier of 8 kJ/mol in the Melius–Blint surface for dissociation of the HO_2 in reaction −1a.[14] Calculations by Dunning et al.[16] reduce this barrier to less than 1.7 kJ/mol. Also for reaction −1 the Melius–Blint surface apparently overestimates the long-range O–OH attraction[17] while the Quack–Troe interpolation scheme[18] leads to better agreement with the experimental values at low temperatures.[19]

In summary, it is encouraging to see that recent microscopic and macroscopic experimental data start to give a more converging picture on this reaction. However, more work should be done on the potential energy surface used for this system. Direct information on the potential energy surface of the HO_2 intermediate can be obtained experimentally by using the laser-induced fluorescence signal generated by transitions to higher repulsive potential energy surfaces.[82] As depicted in Figure 5a, photoemission occurs when the HO_2 wave packet, in the course of its movement on the upper repulsive potential surface, favorably overlaps the HO_2 vibrational levels in the lower (bound) electronic state. Here, the emission to higher vibrational overtones and therefore at longer wavelengths corresponds with later times in the course of photodissociation. Figure 5b shows the experimental arrangement for such measurements, which can give data for the vibrational frequencies of the HO_2 electronic ground state up to the dissociation limit. HO_2 radicals are generated by H-atom addition to O_2 at high pressures by using ArF laser photolysis of

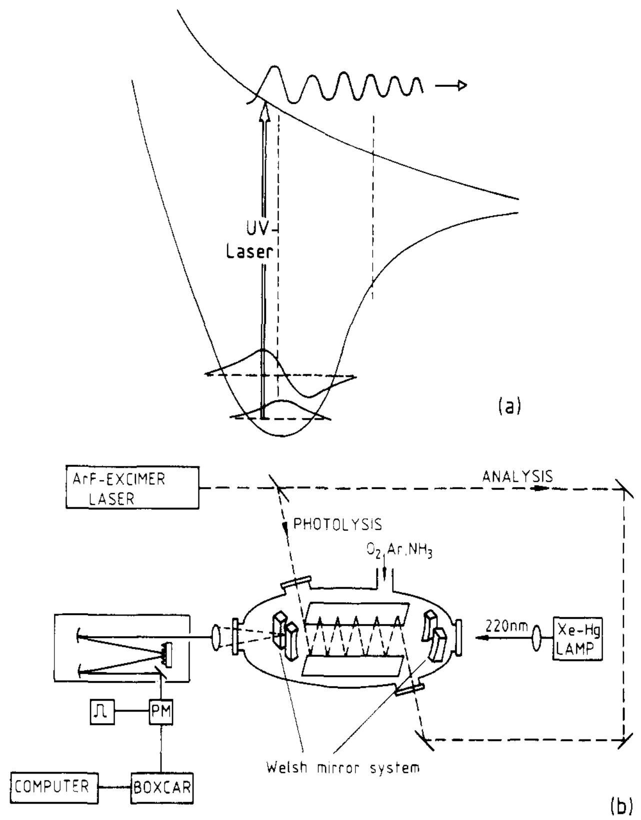

Figure 5. (a) LIF (resonance Raman) spectroscopy of HO_2. (b) Experimental arrangement for LIF (resonance Raman) spectroscopy of HO_2.

NH_3 as the hydrogen atom source. A part of the laser pulse for photolysis is delayed and the frequency shift of the fluorescence lines relative to the excitation wavelength is recorded with a gated multiplier and boxcar system. HO_2 concentrations were measured by UV-absorption spectroscopy. Similar experiments have been carried out for the triatomic molecule O_3 by Kinsey and coworkers.[82] In these experiments a O_3 partial pressure between 300 and 500 mtorr is applied. When powerful ArF excimer lasers are used for NH_3 photolysis in the presence of O_2, HO_2 concentrations in a similar concentration range can be produced by stabilizing the HO_2 complex with argon pressures of several bar. While the transition probabilities for O_3 at 266 nm and HO_2 at 193 nm are similar the ArF excimer laser used here delivers at least an order of magnitude higher intensities than the Nd:YAG laser used in the O_3 experiments. Further experiments for reaction 1 must also be directed to additional thermal rate data measurements in the high-temperature range and measurements of absolute reaction cross sections at different collision energies.

In reaction 2, four atoms with a relatively large number of electrons are involved, making theoretical calculations more difficult. The three lowest electronic states of the HCO_2 radical have been studied by configuration interaction calculations.[20] More recent calculations by Dunning and Harding[21,22] show that the reaction proceeds through an exoergic addition of OH to CO forming the trans isomer of HOCO. Interconversion of the trans and cis isomers of HOCO appears to be a very facile process involving only a low barrier. Product formation is predicted to take place from the cis isomer of HOCO exclusively. While the saddle point for addition of OH to CO is very "early" and broad, the saddle point for elimination of H from HOCO is centrally located and very narrow. The narrowness of the second barrier

---

(14) C. Cobos, H. Hippler, and J. Troe, *J. Phys. Chem.*, **89**, 342 (1985).
(15) J. A. Miller and N. J. Brown, *J. Phys. Chem.*, **86**, 772 (1982).
(16) T. H. Dunning, Jr., S. P. Walch, and M. M. Goodgame, *J. Chem. Phys.*, **74**, 3482 (1981).
(17) S. N. Rai and D. G. Truhlar, *J. Chem. Phys.*, **79**, 6046 (1983).
(18) M. Quack and J. Troe, *Spec. Publ. Chem. Soc.*, **No. 2**, 175 (1977).
(19) N. Cohen and K. R. Westberg, Report No. ATR 82(7888)-3, Aerospace Corp., El Segundo, CA, 1982.
(20) S. P. Peyerimhoff, P. S. Skell, D. D. May, and R. J. Buenker, *J. Am. Chem. Soc.*, **104**, 4515 (1982).
(21) T. H. Dunning, Jr., and L. B. Harding, "Ab Initio Determination of Potential Energy Surfaces for Chemical Reactions", in "Theory of Chemical Reaction Dynamics", M. Baer, Ed., CRC Press, Boca Raton, FL, 1984.
(22) A. F. Wagner and L. B. Harding, Annual Report of the Theoretical Chemistry Group, Argonne National Laboratory, 1983, p 8.

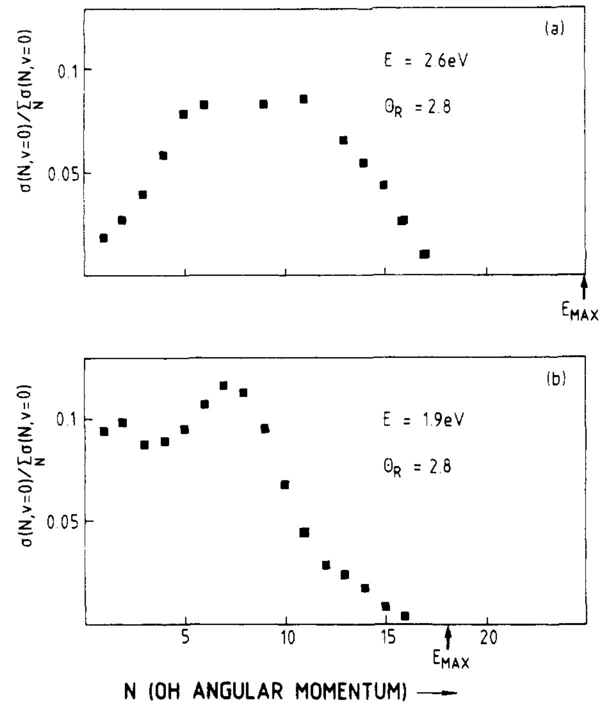

Figure 6. Rotational state distribution for the reaction $H + CO_2 \rightarrow OH + CO$ (2) at 2.6 (a) and 1.9 eV (b) relative collision energy.

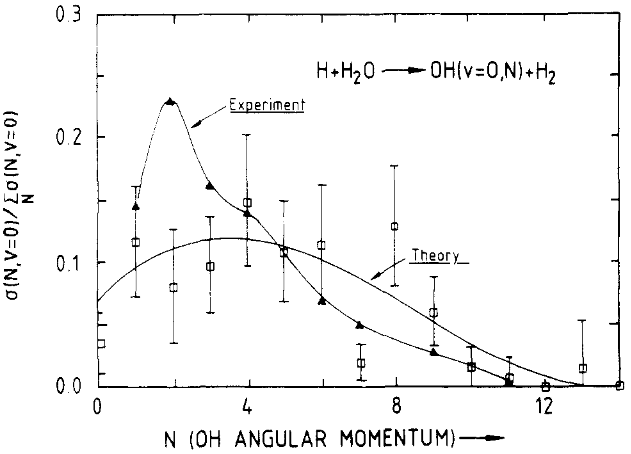

Figure 7. Experimental and theoretical rotational state distributions for the reaction $H + H_2O \rightarrow OH + H_2$ (3) at 2.6-eV collision energy.

can lead to an important contribution to the rate coefficient from quantum mechanical tunneling. If a simple Wigner approximation is used, the calculation shows that the tunneling contribution to the room temperature rate coefficient of reaction −2 is more than 90%.[21] However, more sophisticated tunneling calculations and a variational treatment of transition-state theory should be carried out. Energies for two alternative reaction pathways were calculated also: one indirect route by (1,2)-hydrogen migration from HOCO with a barrier of 25 kJ/mol above the HCO_2 route discussed first and direct insertion of the CO into the OH bond for which a very large barrier of 126 kJ/mol is predicted. Presently, no dynamical calculations are available which can be compared with experiments using translational hot hydrogen atoms[23,24,31] and OH radicals[25] showing substantial rate enhancement with increasing translational energy. Figure 6 shows measurements of the OH rotational distributions from the $H + CO_2$ reaction at 2.6- and 1.9-eV collision energy. Clearly, more experimental and theoretical studies are necessary to understand this key reaction of all hydrocarbon oxidation processes.

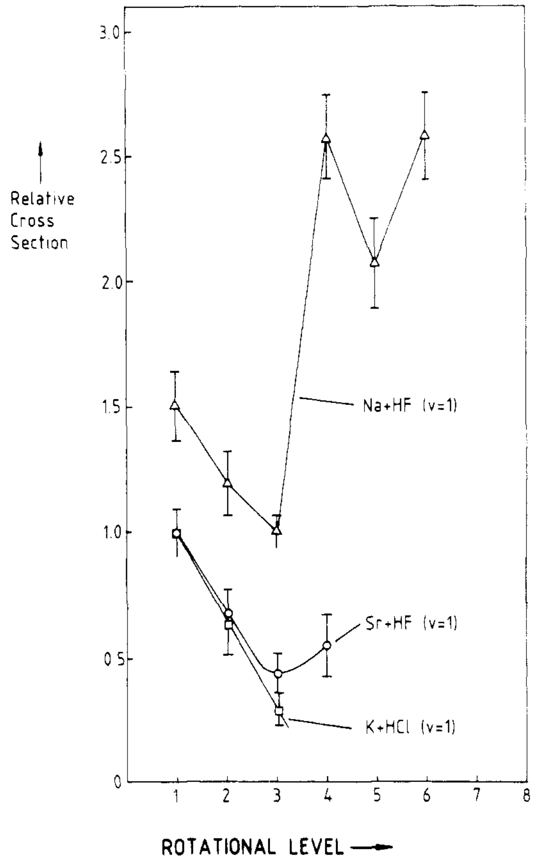

Figure 8. Experimental examples for the variation of total reactive cross sections as function of the rotational quantum number in the reactions $K + HCl(v{=}1,N)$,[34] $Sr + HF(v{=}1,N)$,[35] $Na + HF(v{=}1,N)$.[36]

Experimental and theoretical results are available for reaction 3 with high translational energy of the reactants[2,26,27] using an ab initio potential energy surface.[28] Figure 7 shows the measured and the calculated OH rotational state distributions at 2.6-eV relative collision energy. The experimental[2] reaction cross section is 0.24 ± 0.1 Å^2 compared to calculated[30] 0.28 ± 0.06 Å^2. This surface gives also fairly accurate thermal rate coefficients for reaction 3.[29]

Rotational Excitation

Compared to translational and vibrational excitation, the effect of reactant rotation has been studied experimentally and theoretically in fewer examples. Rotational levels are in most cases very closely spaced and rotational relaxation, especially for low levels, is faster than vibrational relaxation, so that rotational state selection becomes more difficult. Early experimental data were obtained by Polanyi, Bernstein, and co-workers by applying the principle of detailed balance to infrared chemiluminescence data obtained from the reverse exothermic reactions[31] and measuring the depletion of chemiluminescence under arrested relaxation conditions.[32] In a more direct way, Bernstein,[33] Brooks,[34] Zare,[35]

---

(23) G. A. Oldershaw and D. A. Porter, *Nature (London)*, **223**, 490 (1969).

(24) C. R. Quick and J. J. Tiee, *Chem. Phys. Lett.*, **100**, 223 (1983).

(25) A. Jacobs and J. Wolfrum, to be submitted for publication.

(26) H. Elgersma and G. C. Schatz, *Int. J. Quantum Chem. Symp.*, **15**, 611 (1981).

(27) G. C. Schatz, M. C. Colton, and J. L. Grant, *J. Phys. Chem.*, submitted for publication. O. Rashed and M. J. Brown, *J. Chem. Phys.*, **82**, 5506 (1985).

(28) S. P. Walch and T. H. Dunning, Jr., *J. Chem. Phys.*, **72**, 1303 (1980). G. C. Schatz and S. P. Walch, *J. Chem. Phys.*, **72**, 776 (1980).

(29) G. C. Schatz and H. Elgersma, *Chem. Phys. Lett.*, **73**, 21 (1980). D. G. Truhlar and A. D. Isaacson, *J. Chem. Phys.*, **77**, 3516 (1982).

(30) K. Kleinermanns and J. Wolfrum, *Chem. Phys. Lett.*, **104**, 157 (1984).

(31) K. G. Anlauf, D. H. Maylotte, J. C. Polanyi, and R. B. Bernstein, *J. Chem. Phys.*, **51**, 5716 (1969).

(32) B. A. Blackwell, J. C. Polanyi, and J. J. Sloan, *Chem. Phys.*, **24**, 25 (1977).

(33) S. Stolte, A. E. Proctor, and R. B. Bernstein, *J. Chem. Phys.*, **62**, 2506 (1978).

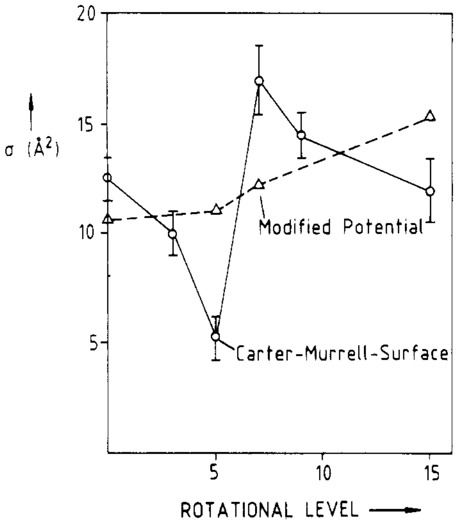

Figure 9. Reaction cross section for Li + HF(v=2,N) at E_T = 36 kJ/mol obtained from QCT calculations[39] using the original fit to ab initio points by Carter and Murrell[39] and a modified[40] potential surface.

Loesch,[36] and co-workers used selective rotational excitation of HCl and HF in a molecular beam with tunable infrared lasers.

Figure 8 shows data for the variation of the total reactive cross section as a function of the rotational quantum number. The results are typical for many direct reactions. The initial decline near threshold of the reaction indicates that the molecular rotation inhibits the reaction. This can be explained by the fact that for many atom plus diatomic reactions the barrier heights depend strongly on the angle of approach. The orientation preferred for the reaction is therefore disrupted by the rotational excitation of the diatomic molecule. At higher values of the rotational quantum number N the reactive cross section increases due to the larger number of product states becoming available and the increasing "cone of acceptance" for reactive collisions. Thus studies of the effect of reagent rotation can give information on the anisotropy of the reactive potential. However, extensive quantitative comparisons between experimental and theoretical results obtained from ab initio potential energy surfaces are still rare. Results for a simple system involving relatively few electrons

$$\mathrm{Li} + \mathrm{HF}(v,N) \rightarrow \mathrm{LiF}(v',N') + \mathrm{H} \qquad (4)$$

are shown in Figure 9. For this prototype alkali-hydrogen halide exchange reaction, an ab initio surface[37] in a form[38] for use in dynamical studies is available. Trajectory studies[39] show, after the monotonic decrease, a sharp increase of the reactive cross section between N = 5 and 7, so that under these conditions reagent rotation would be nearly four times more efficient than vibration causing reaction. However, recent trajectory calculations show[40] that these structures are caused by the wrong asymptotic behavior of the Carter-Murrell surface[38] outside the ab initio points.[37]

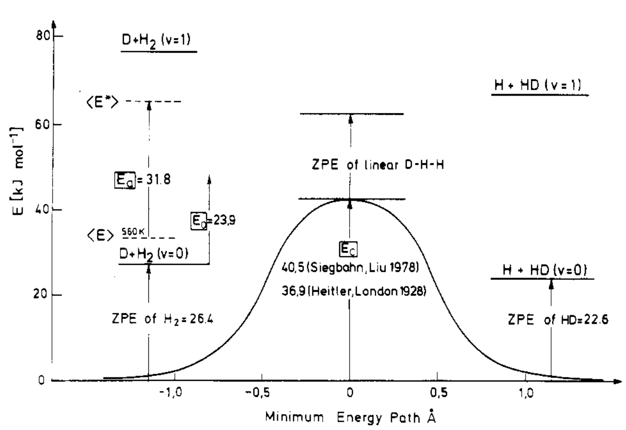

Figure 10. Characteristic energies for reaction 5.

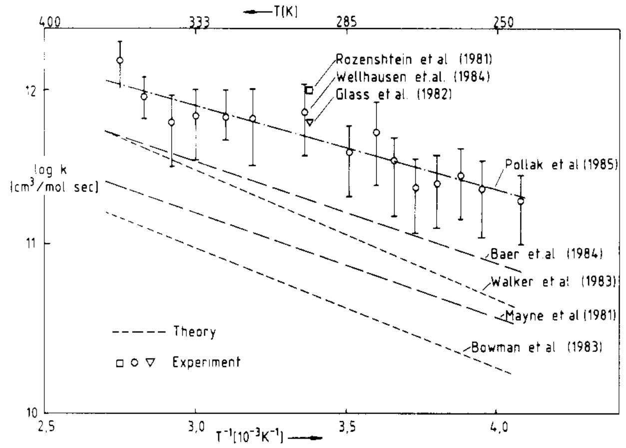

Figure 11. Comparison of experimental and theoretical results for the temperature dependence of the rate of reaction 5, D + H_2(v=1) → HD(v=0,1) + H: Rozenshtein et al.,[44] Glass et al.,[46] Wellhausen et al.,[47] Walker et al.,[50] Mayne et al.,[51] Bowman et al.,[52] Baer et al.,[53] Pollak et al.[55]

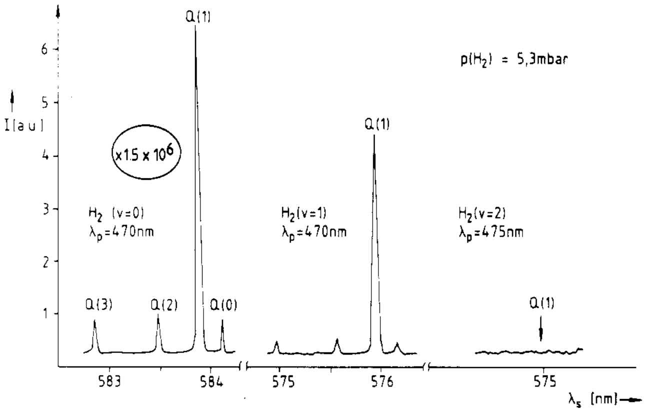

Figure 12. CARS spectra of ground-state and vibrational excited H_2 molecules produced in a microwave discharge.[85]

Vibrational Excitation

The exchange reaction between the hydrogen atom and the hydrogen molecule provides the simplest case where, for neutral species, the effect of vibrational excitation on the kinetic process of bond breaking under the influence of new bond formation can be studied experimentally and theoretically. As shown in Figure 10, single vibrational quantum excitation of the H_2 molecule exceeds the Arrhenius activation energy (E_a), the threshold energy (E_0), as well as the potential energy barrier height (E_c) of the reaction H + H_2. More than half a century ago, London[41] was the first to point out that the potential energy of the H_3 system can be expressed in terms of three Coulombic interaction integrals and three exchange integrals. This simple valence bond calculation leads to a potential energy barrier E_c = 36.9 kJ/mol, not far from the result obtained with modern high-speed electronic computing devices.[42] However, a more precise treatment of the London

---

(34) H. H. Dispert, M. W. Geis, and P. R. Brooks, *J. Chem. Phys.*, **70**, 5317 (1979).

(35) Z. Karny, R. C. Estler, and R. N. Zare, *J. Chem. Phys.*, **69**, 5199 (1978). C. Man and R. C. Estler, *J. Chem. Phys.*, **75**, 2779 (1981).

(36) F. Heismann and H. J. Loesch, *Chem. Phys.*, **64**, 5199 (1978). M. Hoffmeister, L. Potthast, and H. J. Loesch, *Chem. Phys.*, **78**, 4376 (1983).

(37) M. M. L. Chen and H. F. Schaefer III, *J. Chem. Phys.*, **72**, 4376 (1980).

(38) S. Carter and J. N. Murrell, *Mol. Phys.*, **41**, 567 (1980).

(39) I. Noor Batcha and N. Sathyamurthy, *Chem. Phys.*, **77**, 67 (1983).

(40) H. J. Loesch, private communication.

(41) F. C. London, "Probleme der Modernen Physik", Hirzel, Leipzig, 1928, p 104.

(42) P. Siegbahn and B. Liu, *J. Chem. Phys.*, **68**, 2457 (1978). B. Liu, *J. Chem. Phys.*, **80**, 581 (1984).

method including contributions resulting from requisite overlap and three center terms destroys the good, accidental agreement with modern results. Selected ab initio points of the potential energy hypersurface were calculated by Seigbahn and Liu[42] and fitted by Truhlar and Horowitz[43] to an analytical function which represents the potential energy hypersurface mathematically in a smooth and easily manageable way.

Experiments on the effect of vibrational excitation on the rate of hydrogen atom exchange reaction were hampered by the difficulties in preparing and measuring known concentrations of vibrationally excited hydrogen molecules. The methods used include thermal generation of $H_2(v=1)$,[44] energy transfer from laser-excited $HF(v=1)$,[45] and microwave discharge generation of $H_2(v=1)$.[46,47] Results of measurements and calculations on the rate of the reaction

$$D + H_2(v=1) \rightarrow HD(v=0,1) + H \qquad (5)$$

are shown in Figure 11. Figure 12 shows CARS spectra obtained for ground-state and vibrational excited H_2 molecules produced in a microwave discharge[85] for investigation of reaction 5. No indication for the pressure of higher vibrational states above $H_2(v=1)$ under the conditions of the rate measurements could be found.

The central aim of chemical dynamics is the determination of the probability for ending in a defined final state of products from a well-defined initial state of reactants. In the context of quantum mechanics this means: what is the probability that a given initial state, which can be described by a linear combination of eigenfunctions of a system in the reactant region, couples with different product channels described by a linear combination of eigenfunctions in the product region using the "ab initio" calculated potential energy hypersurface? In general, one has to consider a change in the coordinate system in the collision process, since the eigenfunctions of the reactants and products are usually not orthogonal. The probability P_{if} for a transition of the initial state i to the final state f can be described by a transition matrix S_{if}, so that

$$P_{\text{if}} = |S_{\text{if}}|^2$$

The numerical effort of a dynamical calculation increases rapidly with the size of the S-matrix, i.e. the number of coupled states that have to be considered in the dynamical model. Therefore a number of quantum mechanical approximation methods were developed to keep the number of matrix elements as small as possible.

The most accurate approximation is the j_z-conserving or centrifugal-sudden approximation, where certain off-diagonal terms in the kinetic energy expression, which couple the body-fixed projection states, are neglected. However, this approximation still involves a considerable numerical effort. Searching for further simplifications one comes to the rotational sudden approximation, which neglects the coupling between the different rotational states. Although these approximations introduce considerable interventions into the system (the j_z-conserving method interferes with the law of conservation of angular momentum, and the rotational sudden approximation even affects the law of conservation of energy), all the qualitative features of the reaction dynamics are preserved and the introduction of these approximations into the system is the foundation for calculating more complex systems.

Another quantum treatment of reactive scattering is the distorted-wave Born approximation (DWBA). The method involves the solution of a nonreactive elastic scattering problem for reactants on the one side, and the analogous problem on the product side. After that, the transition amplitude is calculated, using the full potential surface. The DWBA approach can relatively easily be generalized to other reactions in three dimensions with the quasiclassical trajectory method and the transition-state theory (TST). Rate constants derived from TST calculations always provide an upper bond of the exact rate constant. To minimize the TST rate some vibrational methods have been developed. The rate of reaction 5 has been calculated with the variety of theoretical methods discussed above.[48-56]

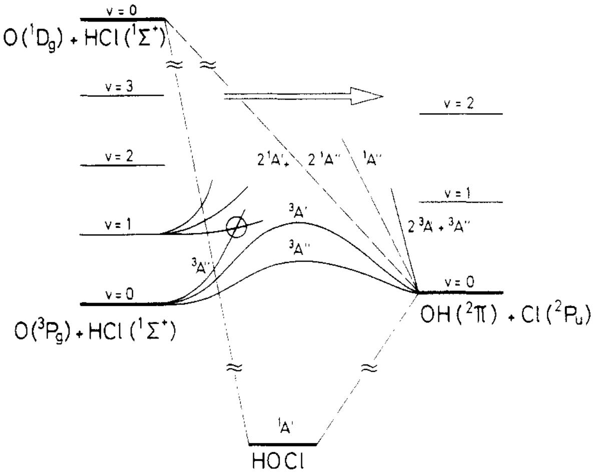

Figure 13. Reaction and vibrational deactivation pathways for $HCl(v)$ in collisions with $O(^3P)$ atoms.

As shown in Figure 11, good agreement between theory and experiments was obtained for a recent calculation by Pollak et al.[55] who interpreted computed IOS reactive cross sections as rotationally averaged cross sections rather than as cross sections for the ground rotational state of the reactants. The interpretation is based on transition state theory arguments.[55] Clearly, further experimental and theoretical work is needed for this reaction which should be the best-understood of all chemical processes.

Rate coefficients for reaction −3 have been measured with vibrational excitation to $v = 1$ for both OH and H_2. While OH excitation leads to negligible rate enhancement,[57] vibrational excitation of H_2 accelerates the rate of reaction −3 by more than two orders of magnitude.[58] The experimental result can be understood by considering the OH bond in agreement with ab-initio calculations of the transition state configuration[59] as a "spectator bond" which remains essentially unchanged during the course of the reaction. Although only a few experimental data on the temperature dependence of the $OH + H_2(v=1)$ reaction are available,[60] it can be concluded that, at elevated temperatures, a substantial part of the reactive flux in the thermal reaction occurs via vibrationally excited states of H_2. Similar results have been obtained from measurements of the temperature dependence of the rate of the reaction $Br + HCl(v=2)$[61] and $^{37}Cl + H^{35}Cl(v=1)$[62,63] using isotopically selective vibrational excitation of HCl

---

(43) D. G. Truhlar and C. J. Horowitz, *J. Chem. Phys.*, **68**, 2460 (1978).

(44) E. B. Gordon, B. I. Iwanov, A. P. Perminow, V. G. Balalaev, A. N. Ponomarev, and V. V. Fitatov, *Chem. Phys. Lett.*, **58**, 425 (1978). V. B. Rozenshtein, Gershenzon, M. Yu., A. V. Ivanow, and S. I. Kucherjavii, *Chem. Phys. Lett.*, **105**, 423 (1984).

(45) M. Kneba, U. Wellhausen, and J. Wolfrum, *Ber. Bunsenges. Phys. Chem.*, **83**, 940 (1979).

(46) G. P. Glass and B. N. Chaturvedi, *J. Chem. Phys.*, **77**, 3478 (1982).

(47) U. Wellhausen, Dissertation Universität Göttingen, 1984. U. Wellhausen and J. Wolfrum, *Ber. Bunsenges. Phys. Chem.*, **89**, 316 (1985).

(48) E. Pollak, *Chem. Phys. Lett.*, **80**, 45 (1981).

(49) E. Pollak and R. E. Wyatt, *J. Chem. Phys.*, **78**, 4464 (1983).

(50) R. B. Walker and E. F. Hayes, *J. Phys. Chem.*, **87**, 1255 (1983).

(51) H. R. Mayne and J. P. Toennies, *J. Chem. Phys.*, **75**, 1794 (1981).

(52) J. M. Bowman, U. T. Lee, and R. B. Walker, *J. Chem. Phys.*, **79**, 3742 (1983).

(53) N. Abu Salbi, D. J. Kouri, Y. Shima, and M. Baer, *Chem. Phys. Lett.*, **105**, 472 (1984).

(54) D. D. Gerrity and J. J. Valentini, *J. Chem. Phys.*, **79**, 5202 (1983).

(55) E. Pollak, N. Abu Salbi, and D. J. Kouri, *Chem. Phys. Lett.*, **113**, 585 (1985).

(56) N. Abu Salbi, D. J. Kouri, M. Baer, and E. Pollak, *J. Chem. Phys.*, submitted for publication.

(57) J. E. Spencer, H. Endo and G. P. Glass, *Symp. (Int.) Combust.*, [*Proc.*], *16th*, *1976*, 829 (1977).

(58) R. Zellner and W. Steinert, *Chem. Phys. Lett.*, **81**, 568 (1981).

(59) S. P. Walch and T. H. Dunnings, Jr., *J. Chem. Phys.*, **72**, 1303 (1980). G. C. Schatz, *J. Chem. Phys.*, **74**, 1133 (1981).

(60) R. Zellner, *J. Phys. Chem.*, **83**, 18 (1979).

(61) M. Kneba, R. Stender, U. Wellhausen, and J. Wolfrum, *J. Mol. Struct.*, **59**, 207 (1980).

(62) M. Kneba and J. Wolfrum, *J. Phys. Chem.*, **83**, 69 (1979).

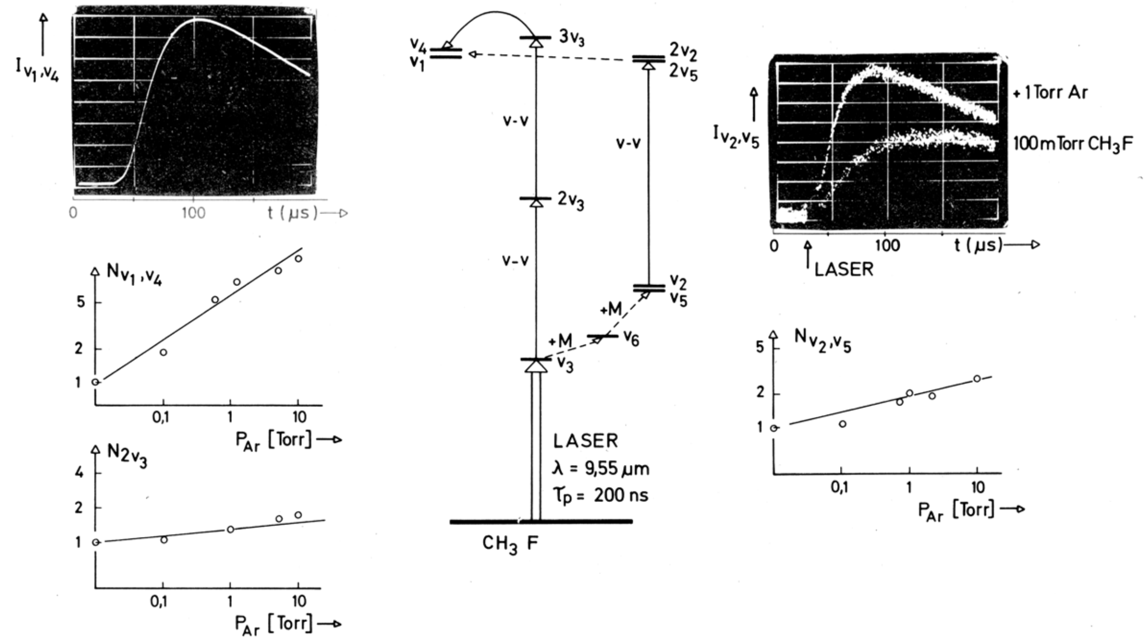

Figure 14. Collision-induced intramolecular energy transfer in CH_3F.

and mass spectrometric detection of the reaction products. However, the effective use of vibrational energy to overcome the potential energy barrier E_c is very restricted in general. Unless the vibrational excitation leads to an substantial increase in the preexponential factor combined with the reduction of the barrier height, the rate increase by vibrational energy is usually cancelled in thermal reactions by the Boltzmann factor. In addition, very efficient vibrational energy transfer may occur in potentially reactive collisions. A theoretical model to explain the effective energy transfer in collisions involving P state atoms as a result of electronically nonadiabatic curve crossing was given by Nikitin and Umanski.[64] As shown in Figure 13, several potential surfaces exist for the interaction of $O(^3P)$ atoms with $HCl(v)$. At certain distances a nonadiabatic coupling between the different vibronic states is possible. Experimental results on the reverse reaction[65] $Cl + OH(v)$ and the observed formation of $OH(v=1)$ from $O(^3P) + HCl(v=2)$[66] indicate that the chemical reaction occurs predominantly vibronically on a triplet surface and does not proceed through a long-lived HOCl complex.

An interesting example in which the effect of vibrational excitation on complex and direct pathways can be observed simultaneously is the radical reaction

$$O(^3P) + CN(v) \xrightarrow{A} CO(v') + N(^4S) \qquad (6)$$

$$\xrightarrow{B} (NCO)^* \rightarrow CO(v'') + N(^2D)$$

Channel A connects the reactants directly with electronically ground-state nitrogen atoms and CO molecules while channel B correlates with the electronic ground state of the NCO radical as intermediate and with electronically excited nitrogen atoms and electronic ground-state CO molecules as products. The deep attractive "well" of the NCO ground state allows an effective energy exchange for several vibrational periods in the collision complex. The reaction energy is therefore distributed on path B in a statistical way among the reaction products.[67] In the direct path A, vibrational energy in the CN radical is mainly transformed into vibrational excitation of the CO product molecule. The experimental results[68] are in good agreement with trajectory calculations.[69] Among other details, the trajectory calculations give also a picture of how the vibrational excitation of $CN(v)$ will influence the rate of reaction 6 on the two different pathways. On the complex path the reaction cross section decreases with increasing vibrational excitation of CN. This can be understood from the standpoint of the unimolecular decomposition of the intermediate NCO complex, which gives an increasing amount of redissociation into reactants with increasing total energy. As mentioned earlier this kind of behavior has been observed experimentally for reaction 2. For the direct path A the opposite trend is observed. The increase in the reactive cross section with vibrational excitation can be rationalized by an "induced attraction":[70] the barrier due to the repulsion between an attacking atom A and the molecule BC in the vibrational ground state will decrease for $BC(v)$ in high vibrational levels, since in the limit of dissociation of BC an attraction exists between the free atoms A and B.

To obtain information about the bimolecular chemical reaction of a polyatomic molecule excited in a specific vibrational mode, one must first try to decouple the vibrational energy exchange from the removal of the excited molecule by interaction with the added reactant. If a low partial pressure of the excited molecules and spectral and time-resolved detection of the infrared emission from the different excited modes are used, direct observation of the energy flow is possible. Substituted methanes are suitable molecules for such investigations. A great deal of information concerning vibration-to-vibration energy transfer has been obtained for the molecule CH_3F, due mainly to the pioneering studies of Flynn and co-workers[71] using laser-induced infrared fluorescence, infrared double resonance, and time-resolved thermal-lensing experiments. A higher detection sensitivity for the laser-induced fluorescence could be achieved in experiments using a Welsh-type mirror system for the collection of the infrared photons and two plane mirrors for multiple reflection of the exciting CO_2-laser beam.[73] This gave an improvement of a factor of 25 compared

---

(63) M. Kneba and J. Wolfrum, *Symp. (Int.) Combust.*, [*Proc.*], *16th*, *1978*, 497 (1979).

(64) E. E. Nikitin and S. Y. Umanski, *Faraday Discuss. Chem. Soc.*, **53**, 1 (1972).

(65) B. A. Blackwell, J. C. Polanyi, and J. J. Sloan, *Chem. Phys.*, **44**, 25 (1977).

(66) J. E. Butler, J. W. Hudgens, M. C. Lin, and G. K. Smith, *Chem. Phys. Lett.*, **58**, 216 (1978). A. Persky and M. Broida, *J. Chem. Phys.*, **81**, 4352 (1984).

(67) J. Troe, *Annu. Rev. Phys. Chem.*, **29**, 223 (1978). M. Quack, *J. Phys. Chem.*, **83**, 150 (1979).

(68) K. J. Schmatjko and J. Wolfrum, *Symp. (Int.) Combust.*, [*Proc.*], *16th*, *1976*, 819 (1977).

(69) K. J. Schmatjko and J. Wolfrum, *Ber. Bunsenges. Phys. Chem.*, **79**, 69 (1975), **83**, 419 (1978).

(70) A. M. G. Ding, L. J. Kirsch, D. S. Perry, J. C. Polanyi, and J. L. Schreiber, *Faraday Discuss. Chem. Soc.*, **55**, 252 (1973).

(71) R. S. Sheorey and G. W. Flynn, *J. Chem. Phys.*, **72**, 62 (1973).

(72) G. Graner, *J. Phys. Chem.*, **83**, 1491 (1979).

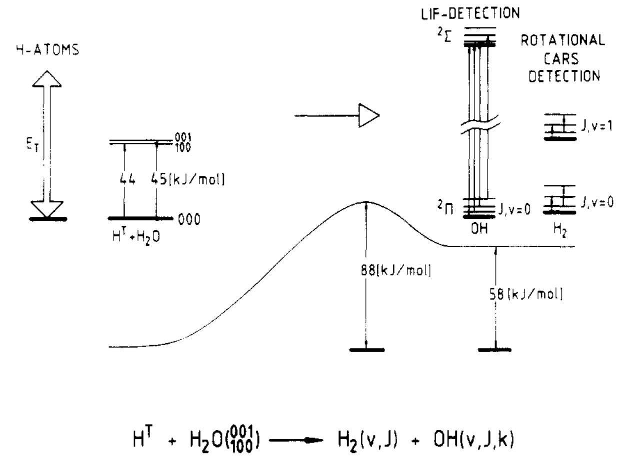

Figure 15. Experimental studies on the effect of selective vibrational and translational excitation in reaction 3.

to fluorescence cells without collecting mirrors. The TEA CO_2 laser used is grating tuned to the P(20) line at 1048.85 cm^{-1} and excites the ν_3 C–F stretching mode of CH_3F. With the CO_2 laser pulses used (200 ns, 500 mJ) a fraction of 0.4 from the CH_3F molecules is excited to the $\nu_3 = 1$ level. After single quantum excitation of the C–F stretching vibration ν_3 at 1049-cm^{-1} vibration energy is transferred first, via "up the ladder" processes in the pumped ν_3 mode. Only four gas kinetic collisions are required in the nearly resonant vibration-to-vibration energy-transfer process. Local Coriolis resonances between the $3\nu_3$ and the ν_4 level at high rotational states[72] allow a small fraction of population in the $2\nu_3$ level to enter the ν_4 level. If the time-resolved fluorescence signals are studied as a function of added inert gas pressure with the partial pressure of CH_3F kept constant, the intensity of the emission from the C–H bending (ν_6, ν_5, ν_2) and C–H stretching (ν_1, ν_4) levels increases drastically (see Figure 14). This can be explained by another dominant pathway under these conditions. The intermode energy gaps between ν_3, ν_6 and ν_2, ν_5 are surmounted in collisions of the excited CH_3F (ν_3) molecules with inert gas atoms. Since the overtone $2\nu_2$ is in Fermi resonance with ν_1, efficient population of the C–H stretching vibrational is also possible. The experiments show that a "metastable" vibrational energy distribution with dominant population in the C–F stretching mode can be created after laser excitation. While the total vibrational energy in the excited CH_3F molecule remains nearly constant the distribution can be changed in a mode selective way by collisions with inert-gas atoms. The reaction

$$Br + CH_3F(\nu_i) \rightarrow HBr + CH_2F \tag{7}$$

has been used as model system for a study of the mode-specific energy consumption in reactions of vibrationally excited polyatomic molecules.[73] The experiments indicate that the C–F vibration ν_3 excited by the laser pulse is much less effective for reaction 7 than C–H vibration populated by collision-induced mode-selective energy transfer.

The effect of vibrational excitation of H_2O in reaction 3 was studied recently by the quasiclassical trajectory method.[27] The reaction rate coefficients are enhanced by exciting any of the vibrational modes of the H_2O molecule. Most of that enhancement is due to a reduction in the threshold energy. The efficiency of threshold reduction varies significantly from mode to mode. The bending mode is the most efficient mode and the asymmetric stretch mode the least. However, there are some ambiguities in the potential energy surface and also some more general difficulties in the application of classical mechanics to polyatomic systems due to the inability of classical mechanics to constrain at least the zero point energy in each mode during the reaction. Experimental studies presently being carried out on the effect of vibrational excitation of H_2O in reaction 3 are illustrated in Figure 15. Selective vibrational excitation of H_2O molecules is achieved by Raman shifting of a tunable dye laser to the infrared. The relative translational energy can be varied continuously by changing the wavelength for photolytic H-atom generation. The product molecules are detected by LIF and rotational-CARS spectroscopy.

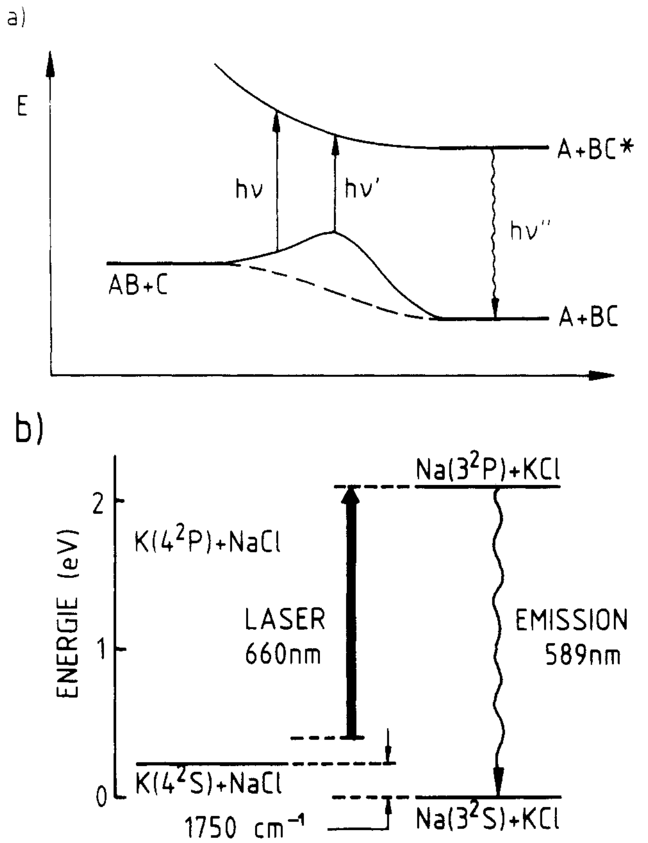

Figure 16. Transition state spectroscopy for the reaction $K(4^2S) + NaCl \rightarrow Na(3^2S) + KCl$ (ref 79).

Electronic Excitation

At some stage in the course of a chemical reaction new bonds are formed and old bonds are broken, so that one has neither "reactants" nor "products". The direct investigation of such "transition states" is the chemist's old dream. Only in recent years has it become possible, with the help of intense laser radiation, to excite these extremely short-lived states (10^{-11} s) electronically and to investigate them spectroscopically, carefully excluding possible artefacts.[75]

Figure 16a shows that a transition state can be excited with a laser wavelength that is nonresonant with the reactant and product states. Among the reactions investigated was that of $K(4^2S)$ atoms with NaCl using excitation with 660-nm laser radiation (Figure 16b) in a crossed molecular beam experiment.[79] As the reaction partners approach, the particle states mutually "disturb" one another and their energy changes until the laser is finally resonant with the $Na^*(3^2P)$–KCl potential curve. Then electronic excitation occurs and light emission from $Na^*(3^2P)$ at 589 nm is observed. Emission at 589 nm occurs even on excitation with light of longer wavelengths. The missing energy comes from the exothermicity of the reaction and thermal energy of the reactants. By improving the signal-to-noise ratio of the mea-

---

(73) K. Kleinermanns and J. Wolfrum, *Laser Chem.*, **2**, 339 (1983).

(74) K. Kleinermanns, G. Marowsky, and J. Wolfrum, to be submitted for publication.

(75) P. R. Brooks, R. F. Curl, and T. C. Maguire, *Ber. Bunsenges. Phys. Chem.*, **86**, 401 (1982).

(76) P. Hering, P. R. Brooks, R. F. Curl, R. S. Judson, and R. S. Lowe, *Phys. Lett.*, **44**, 687 (1980).

(77) H. P. Grieneisen, H. XueJing, and K. L. Kompa, *Chem. Phys. Lett.*, **82**, 421 (1981).

(78) C. Jouvet and B. Soep, *Chem. Phys. Lett.*, **96**, 426 (1983).

(79) T. C. Maguire, P. R. Brooks, and R. F. Curl, Jr., *Phys. Rev. Lett.*, **50**, 1918 (1983).

surements the authors hoped to be able to recognize structures in the spectrum and identify areas of longer residence time of the complex on the ground-state surface from the intensity maxima.

In addition to laser-excited transition states, emission from chemically excited intermediate complexes has also been observed. Polyani et al.[80,81] were able to detect fluorescence from the reaction $F + Na_2 \rightarrow FNaNa^{\pm *} \rightarrow NaF + Na^*(3^2P)$ far from the Na D line. This "wing" fluorescence originates from Na* in the vicinity of NaF (and hence also, for example, from $FNaNa^{+*}$). The higher intensity of the long wavelength "wing" is due to the fact that the upper and lower potential surfaces tend to lie closer together when passing through the intermediate configurations relative to the energy product difference. Although considerable efforts were made, no further structures or resonances were found in these experiments. The actual information on the transition states involved is thus very limited.

Structured transition state spectra were observed by Kinsey et al.[82] after laser photodissociation of ozone at 266 nm. Ozone dissociates within femtoseconds from the upper electronic state of the excited "Hartley" bands to ground-state O_2 and $O(^1D)$.[83] The dissociation is approximately six orders of magnitude faster than the spontaneous emission; nevertheless, fluorescence could be observed. From the frequency shift of the fluorescence lines relative to the excitation wavelength, one obtains vibrational frequencies of the ozone in the electronic ground state up to 500 cm^{-1} below the dissociation limit. The relative line intensities characterize the upper potential surface and the time course of the photodissociation. In a more recent piece of work on the photolysis of CH_3I, Kinsey et al.[84] were able to show that the C–I bond has to be considerably extended before the CH_3 umbrella vibration is excited and the methyl group opens from the tetrahedral geometry in CH_3I to the planar form in the CH_3 product radical. The emission spectrum consists of a long progression in the C–I-stretching vibration ν_3 up to the 29th overtone. Toward longer wavelengths (later times), combination bands between ν_3 and the CH_3 umbrella vibration ν_2 appear. Clearly, the initial movement of the atoms occurs almost exactly along the C–I-stretching vibration coordinate, whereas the CH_3 group opens later to the planar form. At very long wavelengths (high vibrational energies), the bands broaden as a result of the increasing vibrational state density. This picture of the dissociation is in agreement with calculations on the potential surface of the electronically excited CH_3I. Such structured emission spectra of dissociating molecules appear to be extremely promising for obtaining direct and detailed information on transition states of bimolecular chemical reactions.

Acknowledgment. The financial support of the Deutsche Forschungsgemeinschaft is gratefully acknowledged.

Registry No. HO, 3352-57-6; H, 12385-13-6; CO_2, 124-38-9; H_2O, 7732-18-5.

---

(80) P. Arrowsmith, P. E. Bartoszek, S. H. P. Bly, T. Carrington, P. E. Charters and J. C. Polyani, *J. Chem. Phys.*, **73**, 5895 (1980).

(81) P. Arrowsmith, S. H. P. Bly, P. E. Charters, and J. C. Polyani, *J. Chem. Phys.*, **79**, 283 (1983).

(82) D. G. Imre, J. L. Kinsey, R. W. Field, and D. H. Katayama, *J. Phys. Chem.*, **86**, 2564 (1982).

(83) C.-K. Man and R. C. Estler, *J. Chem. Phys.*, **75**, 2779 (1981).

(84) D. G. Imre, J. L. Kinsey, A. Sinha, and J. Krenos, *J. Phys. Chem.*, **88**, 3956 (1984).

(85) T. Dreier, private communication.

Thermodynamics and Kinetics of Carbon–Carbon Bond Formation and Heterolysis through Reactions of Carbocations with Carbanions in Solution

Edward M. Arnett* and Kent Molter

Department of Chemistry, Duke University, Durham, North Carolina 27706 *(Received: July 22, 1985)*

Rate data are presented for the heterolysis of carbon–carbon bonds and their formation through coordination of resonance-stabilized carbocations and carbanions in acetonitrile solution at 25 °C. These rates were determined by NMR line broadening and by the *T* jump technique (in a solution containing 0.48 M supporting electrolyte). Preliminary results are given for a "master equation" to predict some heterolysis energies in solution as a complement to Benson's method for homolysis energies. The results provide for the first time an opportunity to compare the effects of structure variation on the kinetic and thermodynamic properties for such an ostensibly simple reaction in solution. All evidence so far accumulated indicates that these reactions are dominated by ion-solvation factors so that they have little bearing on the gas-phase heterolysis energies. Ionic strength effects and substituent variation suggest that charge development is about half developed at the transition state, but we argue that this cannot be translated simply into pictures of transition-state structure. The results provide a flagrant reversal of the frequently invoked "reactivity selectivity principle" since the most reactive cation is also most selective. On the basis of these results and many others which have appeared recently it may be appropriate to discard the reactivity selectivity principle as a useful principle for either prediction or interpretation.

Introduction

Reaction rates, equilibrium constants, and heats of reaction are perhaps the most fundamental physical observables which manifest reactivity and chemical driving force. The desire of chemists to find relationships between these properties and molecular structure is perennial and has provided much of the motivation for theories of chemical kinetics, especially transition-state theory.

One of Sidney Benson's most valuable contributions has been the development of a predictive scheme for relating homolytic bond energies and free radical stabilities through through the large empirical data bases of heats, entropies and free energies of formation, bond lengths, and bond angles.[1-4] In view of the relatively small solvation energies of molecules and free radicals, homolytic bond energies calculated by Benson's methods, by molecular mechanics, or by quantum mechanics should apply within 1 or 2 kcal/mol to reactions in solution. In fact, the terms *solvation* or *solvation energy* are not to be found in the table of contents or index of ref 1.

---

(1) Benson, S. W. "Thermochemical Kinetics", 2nd ed.; Wiley-Interscience: New York, 1976.

(2) Benson, S. W.; Buss, J. H. *J. Chem. Phys.* **1957**, *29*, 546.

(3) Benson, S. W. "The Foundations of Chemical Kinetics"; McGraw-Hill: New York, 1960.

(4) Benson, S. W. *J. Chim. Phys.* **1979**, *76*, 791.

0022-3654/86/2090-0383$01.50/0